Structural Engineering and Mechanics, Vol. 46, No. 3 (2013) 337-352
DOI: http://dx.doi.org/10.12989/sem.2013.46.3.337

Seismic fragility evaluation of piping system installed in critical structures

Bu Seog Ju[1], Woo Young Jung[2] and Yong Hee Ryu[*1]

[1]*Depatment of Civil Engineering, North Carolina State University, Raleigh, USA*
[2]*Department of Civil Engineering, GangNeung-WonJu National University, GangNeung, Korea*

(Received July 10, 2012, Revised April 5, 2013, Accepted April 9, 2013)

Abstract. Seismic performance of critical facilities has been focused on the structural components over the past decade. However, most earthquake damages were observed to the nonstructural components during and after the earthquakes. The primary objective of this research was to develop the seismic fragility of the piping system incorporating the nonlinear Tee-joint finite element model in the full scale piping configuration installed in critical facilities. The procedure for evaluating fragility curves corresponding to the first damage state was considered the effects of the top floor acceleration sensitivities for 5, 10, 15, and 20 story linear RC and steel building systems subjected to 22 selected ground motions as a function of ground motion uncertainties. The result of this study revealed that the conditional probability of failure of the piping system on the top floor in critical facilities did not increase with increased level of story height and in fact, story level in buildings can tune the fragilities between the building and the piping system.

Keywords: fragility; seismic performance; Tee-joint; probability; uncertainty

1. Introduction

The construction cost of nonstructural components and systems such as mechanical and electrical equipments, medical equipments, plumbing and piping systems encompass relatively higher percentage of total construction cost for critical structures such as nuclear power plants, hospital buildings, high-tech factories, and emergency management building systems. A study from Reitherman (2009) revealed that at least 70% of the total cost for all building occupancies was invested in the nonstructural components and systems, suggesting that the functionality of the structures depended on significantly the functionality of the nonstructural components during and after the earthquake. Over the past two decades, it had been observed that the nonstructural components were much more vulnerable than the structural systems during an earthquake. In some case, damage or failure to the nonstructural components also resulted in direct or indirect injuries and loss of life.

For example, the earthquake in 1994 at Northridge caused no structural damage on the Olive View Medical Center in Sylmar, CA. Instead, the water leakage from broken fire protection sprinkler piping system as well as the chilled water systems in the Medical Center led to greater

*Corresponding author, Ph.D., E-mail: yryu@ncsu.edu

damage by shutting down the structures, which in turn, forced patients to evacuate (Reitherman *et al*. 1995). Furthermore, of the approximate $6.3 billion of direct economic loss to non-residential buildings during 1994 Northridge earthquake, only about $1.1 billion was due to structural damage (Kircher 2003). Northridge earthquake is one example that showed the significantly higher economic loss due to non-structural damage in comparison to structural damage.

A reduction of damage to nonstructural components or an improvement the performance of nonstructural components such as piping systems and Heating, Ventilating, and Air Conditioning (HVAC) systems has emerged as key areas of research in the recent year. Maragakis *et al.* (2003) conducted shake table experiment on cable-brace and unbraced welded hospital piping system. The objective of their shake table test was to identify the capacity characteristics of a hospital piping system with and without bracings as well as system's critical locations. Kafali and Grigoriu (2003) evaluated seismic fragility for a water supply tank and a power generator system in critical facilities with an emphasis of fragility surface evaluation for nonstructural systems. They improved the nonstructural systems by evaluating dampers subjected to seismic ground motions and by reducing computational effort for the fragility analyses by crossing theory for stochastic processes rather than the Monte Carlo method. ATC-58 (Bachman *et al.* 2004) project emphasized the need to address a performance-based design with statistical approaches in nonstructural system supported by structures. Therefore, the study of the annual probability of failure for the systems can be a critical issue to mitigate seismic risk and achieve reliable design.

This research focused on understanding the seismic performance of piping systems installed in critical structures. More specifically, it was targeted on evaluating piping system-level fragilities by characterizing the piping performance using results from experimental test on piping components such as threaded Tee-joints, validating analytical models using experimental results, and then conducting simulations for complete piping system configurations to evaluate system fragilities. Further, the effects of filtering the earthquake motion through the top floor of typical Reinforced Concrete (RC) and steel building systems on the piping fragilities were evaluated.

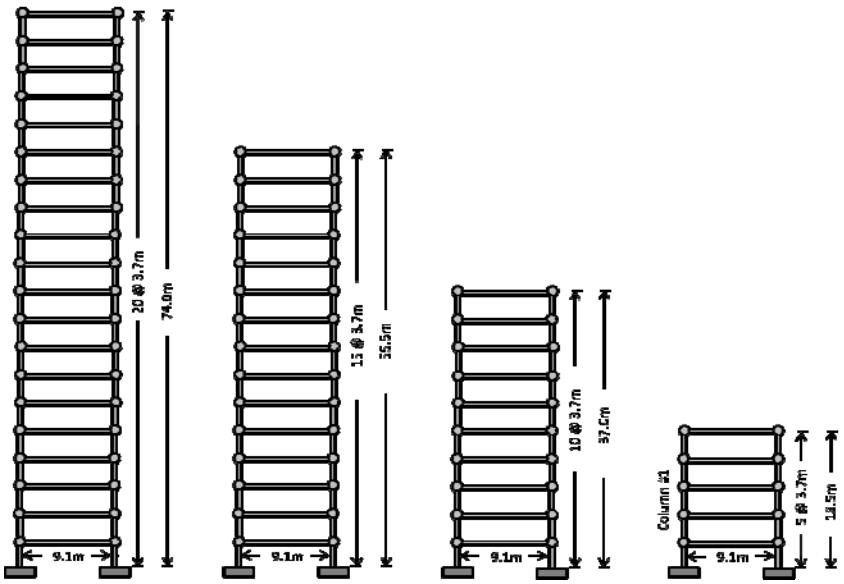

Fig. 1 Linear RC building design model

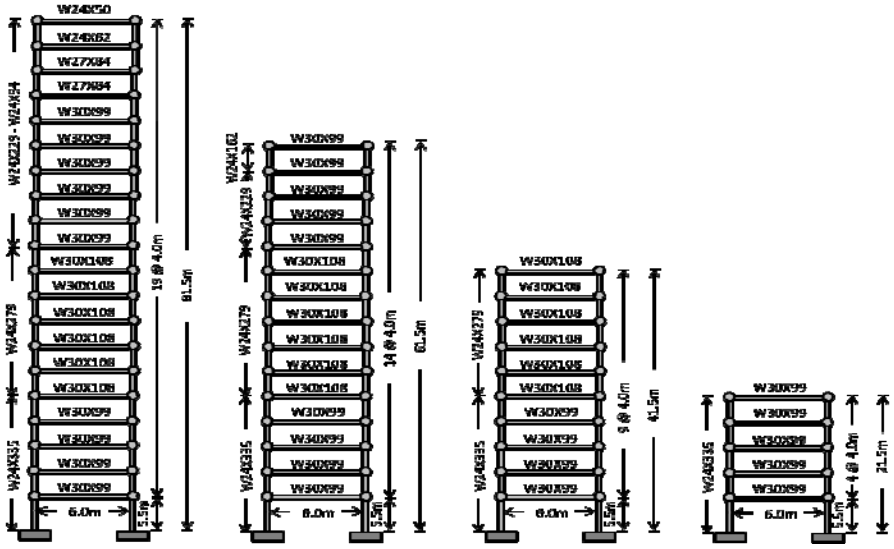

Fig. 2 Linear steel building design model

Table 1 RC building design details: beam sections

Floor	5-Story			10-Story			15-Story			20-Story		
Level	*b (cm)*	*h (cm)*	*f_c'(MPa)*	*b (cm)*	*h (cm)*	*f_c'(MPa)*	*b (cm)*	*h (cm)*	*f_c'(MPa)*	*b (cm)*	*h (cm)*	*f_c'(MPa)*
Level 1 to level 5	81.3	81.3	34.5	81.3	81.3	34.5	81.3	81.3	34.5	81.3	81.3	34.5
Level 6 to level 10				81.3	81.3	34.5	81.3	81.3	34.5	81.3	81.3	34.5
Level 11 to level 15							76.2	76.2	34.5	76.2	76.2	34.5
Level 16 to level 20										61.0	71.1	34.5

2. Description of linear RC and steel frame building design

Four stories of building system were selected (5, 10, 15, and 20 story) for this study as they were previously reported as representative of low-rise, mid-rise and high-rise building systems (Wood *et al*. 2009) in order to simulate different earthquake ground excitations. The building systems using a strong column and weak beam frame design philosophy have been modeled in Open System for Earthquake Engineering Simulation (OpenSees 2010) based on structural analysis of finite element method by Tcl/Tk interpreter extension. Figs. 1 and 2 showed a schematic linear design of 5, 10, 15, and 20 story RC and steel frame building systems. For the simplicity of the analysis, only a single bay system was adopted. The span of the single bay was

Table 2 RC building design details: column sections

Floor Level	5-Story			10-Story			15-Story			20-Story		
	b (cm)	*h (cm)*	*f_c'(MPa)*	*b (cm)*	*h (cm)*	*f_c'(MPa)*	*b (cm)*	*h (cm)*	*f_c'(MPa)*	*b (cm)*	*h (cm)*	*f_c'(MPa)*
Level 1 to level 5	91.4	91.4	68.9	91.4	91.4	68.9	91.4	91.4	68.9	91.4	91.4	68.9
Level 6 to level 10				91.4	91.4	68.9	91.4	91.4	68.9	91.4	91.4	68.9
Level 11 to level 15							86.4	86.4	68.9	86.4	86.4	68.9
Level 16 to level 20										81.3	81.3	68.9

Table 3 Steel building design details: beam and column sections

Floor Level	5-Story		10-Story		15-Story		20-Story	
	Beam	Column	Beam	Column	Beam	Column	Beam	Column
1	W24x335	W30x99	W24x335	W30x99	W24x335	W30x99	W24x335	W30x99
2	W24x335	W30x99	W24x335	W30x99	W24x335	W30x99	W24x335	W30x99
3	W24x335	W30x99	W24x335	W30x99	W24x335	W30x99	W24x335	W30x99
4	W24x335	W30x99	W24x335	W30x99	W24x335	W30x99	W24x335	W30x99
5	W24x335	W30x108	W24x335	W30x108	W24x335	W30x108	W24x335	W30x108
6			W24x279	W30x108	W24x279	W30x108	W24x279	W30x108
7			W24x279	W30x108	W24x279	W30x108	W24x279	W30x108
8			W24x279	W30x108	W24x279	W30x108	W24x279	W30x108
9			W24x279	W30x108	W24x279	W30x108	W24x279	W30x108
10			W24x279	W30x108	W24x279	W30x108	W24x279	W30x108
11					W24x279	W30x99	W24x279	W30x99
12					W24x229	W30x99	W24x229	W30x99
13					W24x229	W30x99	W24x229	W30x99
14					W24x229	W30x99	W24x229	W30x99
15					W24x162	W30x99	W24x162	W30x99
16							W24x162	W30x99
17							W24x162	W27x84
18							W24x117	W27x84
19							W24x117	W24x62
20							W24x94	W21x50

designed as width 9.14 (m) by height 3.66 (m) and width 6.10 (m) by height 3.96 (m) for RC and steel building systems, respectively. The details of this building design can be found in Table 1-3. Both the linear frame building systems were assumed to be fixed at their base, as the soil and structure interaction effects were not considered in this study.

2.1 Numerical modeling of linear frame building model

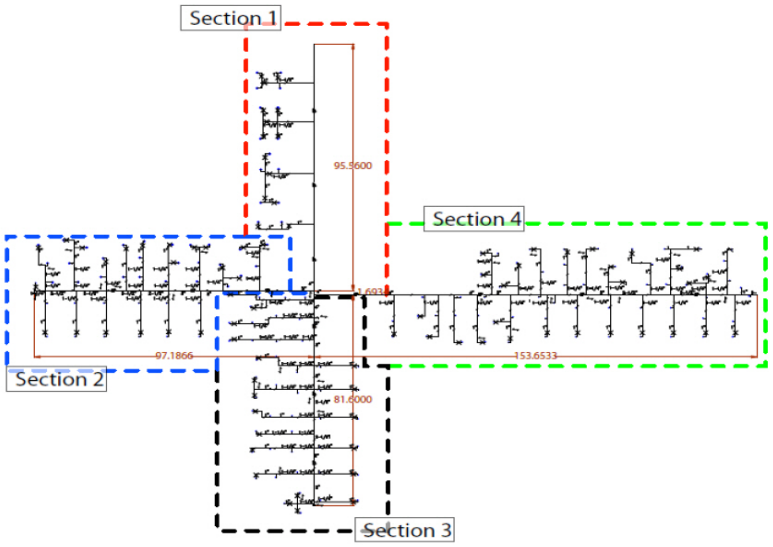

Fig. 3 Real piping system layout

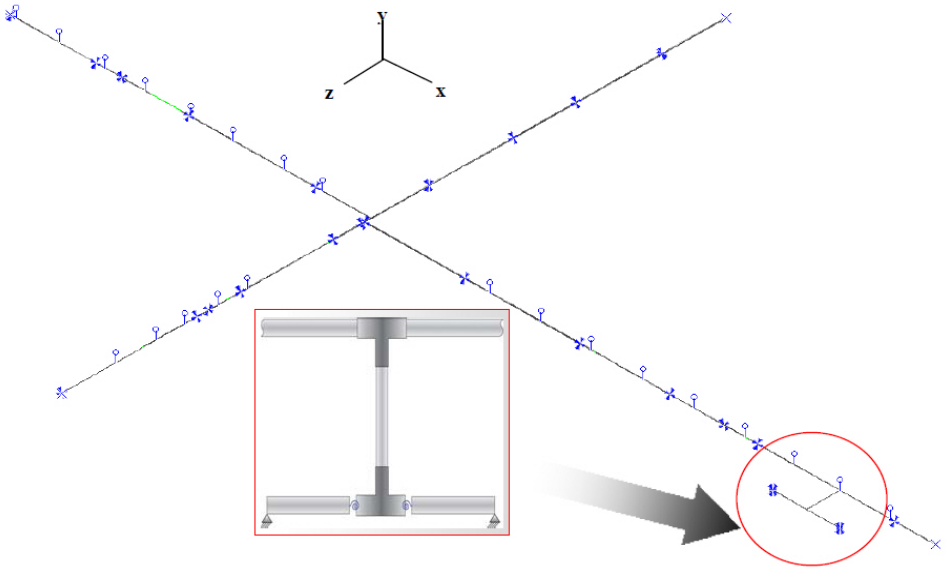

Fig. 4 Piping system configuration for fragility analysis

The numerical discretization of RC and steel frame building models was proposed with an elastic uniaxial material. The *elastic Beam-Column* element in OpenSees was designed to characterize the responses from the beam and column section under earthquake ground motions. Lumped mass and equivalent loads were used for 2-D frame building models. The damping ratio using mass and stiffness proportional Rayleigh damping in all modes distributing to the response in RC and steel frame models was taken as 5% and 2%, respectively.

Table 4 The natural frequencies and mass participation of RC building models

Mode	5-Story		10-Story		15-Story		20-Story	
	Frequency (Hz)	Mass P. (%)	Frequency (Hz)	Mass P. (%)	Frequency (Hz)	Mass P. (%)	Frequency (Hz)	Mass P. (%)
1	2.6200	78.62	1.2008	77.75	0.7505	76.08	0.5258	73.25
2	9.1709	12.42	3.8782	11.12	2.3045	11.91	1.5633	13.85
3	19.1520	5.34	7.3258	4.26	4.2552	4.18	2.8453	4.13
4	32.3346	2.69	11.6042	2.47	6.4823	2.24	4.2406	2.48
5	44.863	0.93	16.9301	1.61	9.0318	1.45	5.8636	1.37

Table 5 The natural frequencies and mass participation of steel building models

Mode	5-Story		10-Story		15-Story		20-Story	
	Frequency (Hz)	Mass P. (%)	Frequency (Hz)	Mass P. (%)	Frequency (Hz)	Mass P. (%)	Frequency (Hz)	Mass P. (%)
1	2.5891	78.37	1.1607	76.37	0.7067	73.71	0.4781	69.44
2	9.0643	12.72	3.8069	12.33	2.2809	14.15	1.4962	16.76
3	18.9214	5.32	7.2670	4.33	4.3521	4.16	2.8427	4.67
4	31.7773	2.67	11.4385	2.45	6.5094	2.28	4.1614	2.28
5	43.9532	0.92	16.4600	1.61	8.9999	1.44	5.6415	1.63

3. Piping system layout

The piping system (Fig. 3) suggested from Ju *et al*. (2011) consisted of main piping running along 4 sections as shown with 64 branches in all. Essentially, main piping system was made of 2-inch to 4-inch pipes, while the branches comprise of pipes with smaller diameter than those of main pipes. This system was supported by unbraced single hangers, transverse braced hangers and longitudinal braced hangers and also, there are 4 anchors at the end of the main piping system.

The fundamental frequency of the original piping system was 0.646 (Hz). From a time history analysis applied to Z-direction of XZ-plane (horizontal direction and El-Centro earthquake normalized to PGA-1g), it is shown in Fig. 3 that the maximum displacement was observed to be 66.38 (cm) in section 3. Therefore, the first system was flexible and the maximum displacement became large. The second model based on NFPA-13 (2007) and SMACNA (2003) design guidelines were also considered in this study (Fig. 4). The particular location of a branch piping system, 2-inch diameter schedule 40 black iron pipe was considered as the critical location for detailed seismic fragility evaluation associated with the results from a linear time history analysis of the complete piping system in the second piping model.

4. Numerical eigenvalue analysis of the building and piping system

Tables 4 and 5 showed the fundamental natural frequencies conducted by an eigenvalue analysis for all RC and Steel linear building models. As can be seen in modal frequencies of the vibrations, the 5-story was much stiffer than other models for both building systems and as the story level for all building models increases the system was more flexible. Tables 4 and 5 also illustrated the mass participation of each building system. Further, Table 6 showed the natural frequencies of the piping system, in which the first and second mode of the piping system was 1.82 Hz and 3.142 Hz, respectively.

Table 6 The natural frequencies of the piping system

Piping System			
Mode	Frequency (Hz)	Mode	Frequency (Hz)
1	1.8190	3	3.2961
2	3.1422	4	3.3295

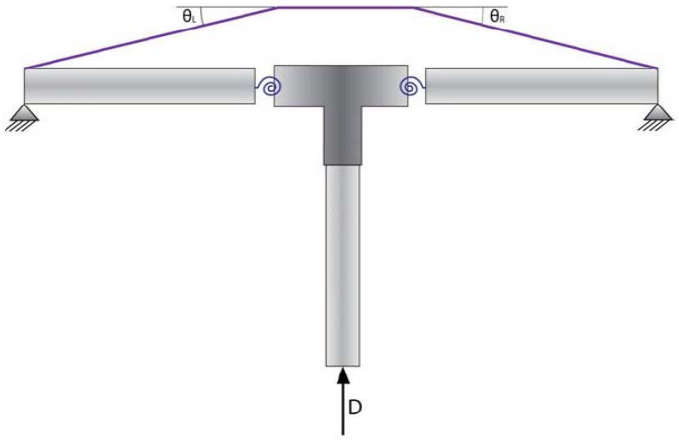

Fig. 5 Nonlinear FE model of the threaded Tee-joint

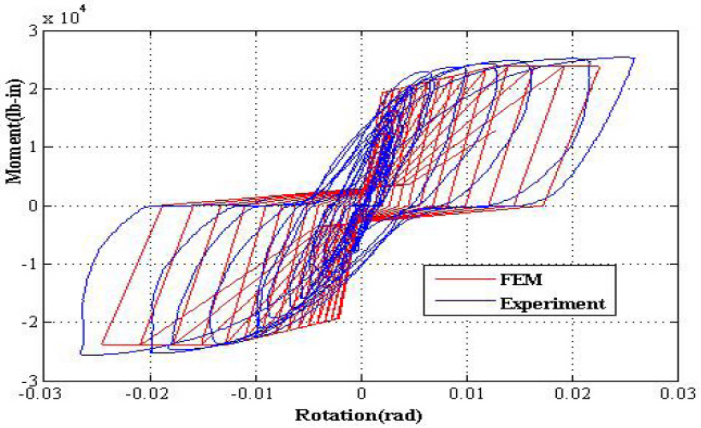

Fig. 6 Verification of the nonlinear Tee-joint FE model at the left spring based on the experimental result conducted by UB

5. Validation of finite element model of the threaded Tee-joint

The nonlinear moment-rotation relationship obtained from cyclic experimental data conducted by University at Buffalo (UB) (Dow 2010) was used to create the nonlinear Finite Element (FE) model of a threaded Tee-joint in 2-inch Black Iron branch piping system. In order to model the Tee-joint system, the *Pinching4* uniaxial model was applied in *OpenSees* Platform. The *Pinching4* material model was able to represent stiffness degradation, strength degradation, and unloading/reloading condition under cyclic loading. Specifically, *Pinching4* material model was

described with positive/negative envelopes of load-deformation response and simulated with strength and stiffness degradation parameters (Mazzoni *et al*. 2006). FE model based on two nonlinear rotational springs and verification of the FE model for the threaded Tee-joint were described in Figs. 5-6, respectively. Further details for FE model can be found in Ju *et al*. (2011).

6. Limit state validation of finite element model of the threaded Tee-joint

In order to evaluate the seismic fragility of the piping system, it was necessary to characterize the limit state criteria corresponding to the damage, as previously suggested by Ju *et al*. (2011). The ASME Boiler Pressure Vessel and Piping Code (2004) defined the rotation corresponding to plastic collapse of piping components using the "Twice the Elastic Slope" (TES) criteria. According to the TES rule, the rotation corresponding to the plastic collapse θ_φ can be determined by the abscissa of the point at which a line with twice the elastic slope intersects the moment-rotation curve. It can be found in Fig. 7 where $\varphi = 2\theta$.

In Fig. 8, the rotations of the left-spring (given in Table 7) corresponding to "First-Leak" damage state during the three cyclic tests were plotted along with the moment-rotation relationship from the experiment. It can be seen that all the 3 failure rotations lie between the lines $\varphi = 2\theta$ and $\varphi = 2.5\theta$ where θ is the elastic slope. From this, we can conclude that the TES ($\varphi = 2\theta$) criteria can be conservatively assumed as the limit state corresponding to "First Leak". However, the same argument can be extended to define other damage states in terms of the elastic slope. Table 8 listed various damage states considered for structural fragility analysis of Tee-joint system.

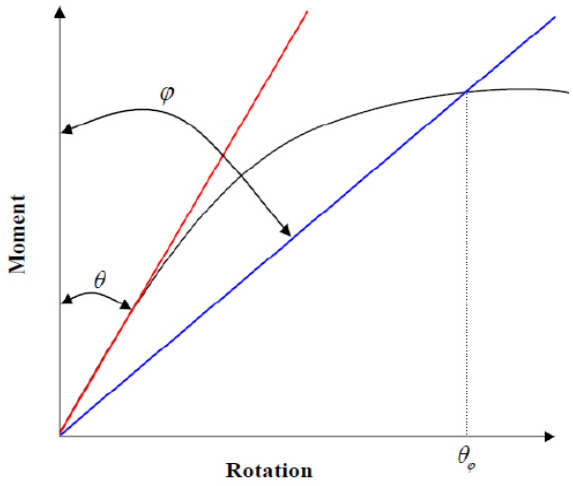

Fig. 7 Twice the elastic slope (TES) criteria

Table 7 Maximum rotations at first leakage point under cyclic tests

Cyclic Test	Rotation (rad)
1	0.0171
2	0.0152
3	0.0142

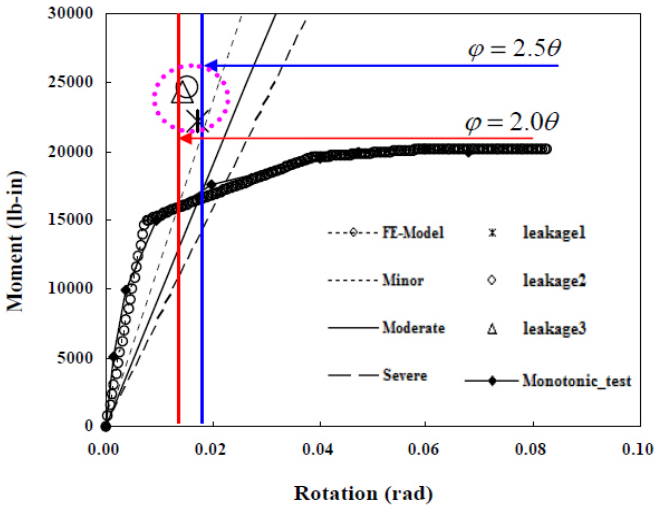

Fig. 8 Damage state corresponding to the first leakage point under cyclic tests

7. Seismic fragility of piping system

The structural and nonstructural system or components of seismic fragility was defined as the conditional probability that a component of a given type would reach or exceed a particular damage state as a function of Engineering Demand Parameter (EDP). The study primarily addressed fragility function generated by the lognormal cumulative distribution function (Porter *et al*. 2006). In recent years, many researchers have conducted the seismic fragility analysis in various structural and nonstructural systems. For example, Pagnini *et al.* (2011) studied the seismic fragility assessment of old masonry building using Monte-Carlo simulation accounting for various uncertainties such as building parameters, model error, and seismic events in demand. Ghosh and Padgett (2012) evaluated the seismic fragility for acing and deterioration of concrete highway bridges under different environmental exposure conditions.

In this study, Eq. (1) gives the expression for fragility at a Peak Ground Acceleration (PGA) level of λ.

$$P_f(\lambda) = P\left[\theta \geq \theta_{\lim} \mid PGA = \lambda\right] \tag{1}$$

The system-level fragility function was estimated empirically by conducting multiple nonlinear time history analyses of the structure for various ground motions.

$$P_f(\lambda) = \frac{\sum_{i=1}^{N} 1\left(\theta_{i,\lambda} \geq \theta_{\lim} \mid PGA = \lambda\right)}{N} \tag{2}$$

In Eq. (2), $\theta_{i,\lambda}$ is the maximum rotation from i^{th} earthquake time history analysis at a Peak Ground Acceleration (PGA) level of λ and 1(.) is the indicator function. We proceeded to evaluate the fragility of the Tee-joint system of 2 in. black iron piping system, when it was a branch of a full scale fire protection piping system.

Table 8 Damage state of the piping system for fragility analysis

Damage State	Definition	θ_{φ} (radians)
Minor Damage (First Leak)	$\varphi = 2\theta$	0.0135
Moderate Damage	$\varphi = 2.5\theta$	0.0175
Severe Damage	$\varphi = 3\theta$	0.0217

Table 9 Earthquake ground motions for fragility analysis

No.	Date	Seismic Events	Locations	Magnitude (M_w)	NPTs	PGA (g)
1	January 17 1994	Northridge	Beverly Hills, USA	6.7	2999	0.5165
2	January 17 1994	Northridge	Canyon Country, USA	6.7	1999	0.482
3	November 12 1999	Duzce	Bolu, Turkey	7.1	5590	0.8224
4	October 16 1999	Hector Mine	Hector	7.1	4531	0.3368
5	October 15 1979	Imperial Valley	Delta	6.5	9992	0.3511
6	October 15 1979	Imperial Valley	El Centro Array #11	6.5	7807	0.3796
7	January 16 1995	Kobe	Nishi-Akashi Japan	6.9	4096	0.5093
8	January 16 1995	Kobe	Shin-Osaka Japan	6.9	4096	0.2432
9	August 17 1999	Kocaeli	Duzce	7.5	5437	0.3579
10	August 17 1999	Kocaeli	Arcelik	7.5	6000	0.2188
11	June 28 1992	Landers	Yermo Fire Station	7.3	22000	0.2448
12	July 23 1992	Landers	Coolwater	7.3	11186	0.4169
13	October 18 1989	Loma Prieta	Capitola	6.9	7991	0.5285
14	October 18 1989	Loma Prieta	Gilroy Array	6.9	7989	0.5550
15	July 20 1990	Manjil	Manjil, Iran	7.4	2675	0.5146
16	November 24 1987	Superstition Hills	El Centro IMP Co Center	6.5	7999	0.3579
17	November 24 1987	Superstition Hills	POE Road	6.5	2230	0.4463
18	April 25 1992	Cape Mendocino	Rio Dell Overpass FF	7.0	1800	0.5489
19	September 20 1999	Chi-Chi	CHY 101, Taiwan	7.6	18000	0.4401
20	September 20 1999	Chi-Chi	TCU045, Taiwan	7.5	16875	0.5120
21	February 09 1971	San Fernando	LA Hollywood Stor Lot	6.6	2800	0.2099
22	January 17 1994	Northridge	Beverly Hills 14145 Mulh	6.7	2999	0.5165

8. Seismic fragility evaluation of piping system at a single location

In order to evaluate seismic fragility of piping system at a single location of the threaded Tee-joint, 22 earthquake set *(N)* as a function of ground motion uncertainty obtained from PEER-NGA (2009) was applied. As shown in Table 9, the selected seismic events were greater than M_w 6.0 and were geographically distributed. The seismic fragility can be also evaluated as follows:

Step 1: 22 earthquake ground motions are normalized to the same level of PGA

Step 2: Apply 22 normalized ground motions to each RC and steel linear building model and then obtain acceleration time histories from each top floor for all building models at the given PGA levels.

Step 3: Apply these acceleration time histories to the FE model of piping system and record the maximum rotation at the Tee-joint in each case.

Step 4: Evaluate seismic fragility of piping system using Eq. (2) at the Tee-joint.

In this study, nonlinear analyses were conducted at various PGA levels from 0.2g to 3.0g at an

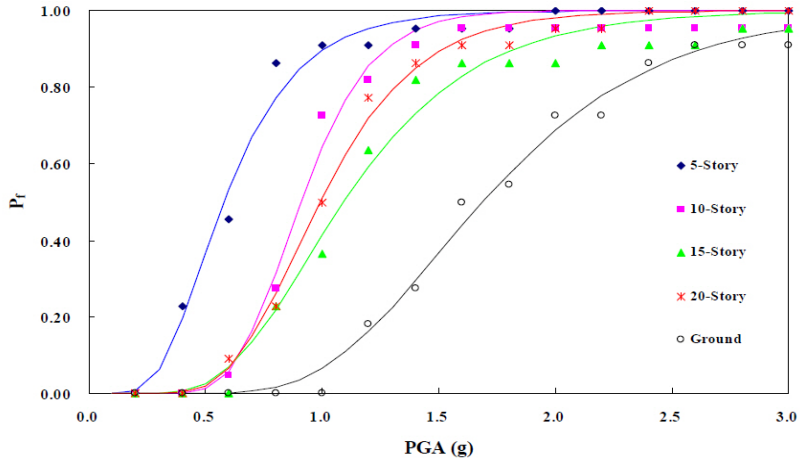

Fig. 9 Seismic fragilities of piping system on the top floor in RC building models

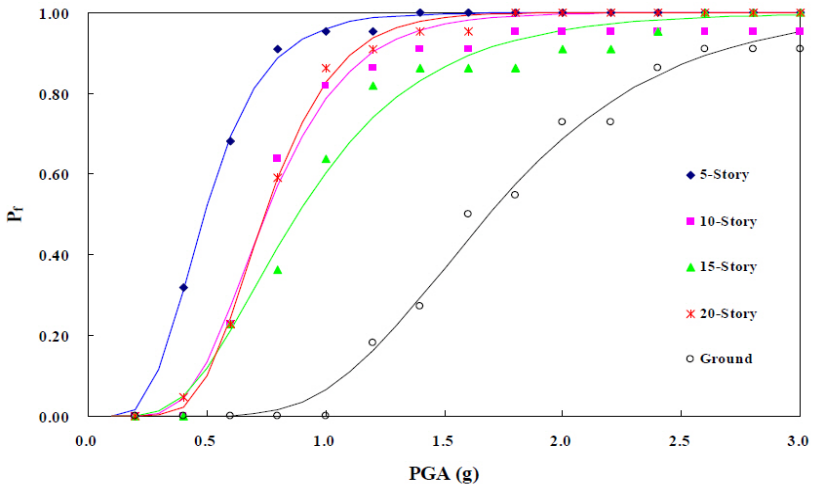

Fig. 10 Seismic fragilities of piping system on the top floor in steel building models

Table 10 Median peak ground acceleration for all building models

Story Level	RC Building Model	Steel Building Model
	Median Peak Ground Acceleration (g)	Median Peak Ground Acceleration (g)
5	0.58	0.49
10	0.91	0.75
15	1.10	0.89
20	0.99	0.75

interval 0.2g and the fragilities corresponding to the first leak damage state (0.0135*rad*) specified in Table 8 were described in Figs. 9-10. As can be seen in the both figures, the fragilities on piping system for 5-story RC and steel linear building system were the most fragile and the piping system on the top floor of 15-story building systems had the smallest probabilities at the given PGA levels. Consequently, the fragilities corresponding to the first damage state on the piping system

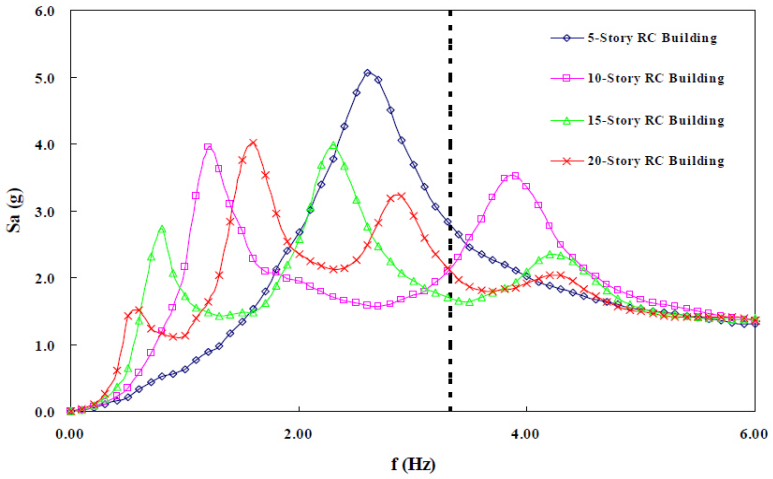

Fig. 11 Mean response spectra on the top floor for RC building models

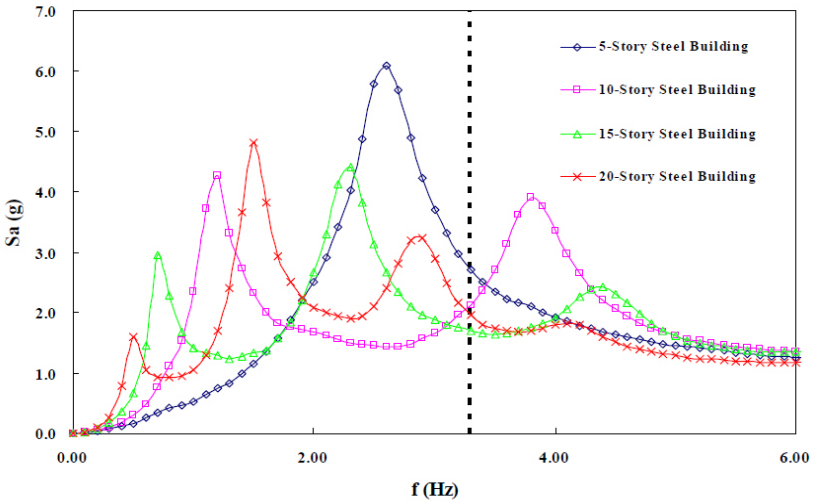

Fig. 12 Mean response spectra on the top floor for steel building models

did not increase with increasing story levels in the building system and the fragilities on the piping system of steel linear building models were slightly higher than those of RC linear building systems. For the better explanation for this output, each top floor mean spectra for 22 earthquake set of all building models were generated in Figs. 11-12. Additional vertical line was in the second mode frequency (3.14Hz), the most critical mode for the piping system. As seen in Fig. 12, the response spectral acceleration in 5-story building for both RC and steel linear building systems showed the highest value. On the other hand the response spectral acceleration in 15-story for RC and steel linear building models received the smallest response spectral acceleration at the second mode frequency of the piping system. Therefore, the piping system in the 5-story linear building system was considered the most vulnerable but the median peak ground acceleration, failure probability of 50 percent of the piping system showed the highest value (1.10g and 0.89g) in the 15-story linear RC and steel building systems given in Table 10. In particular, the conditional

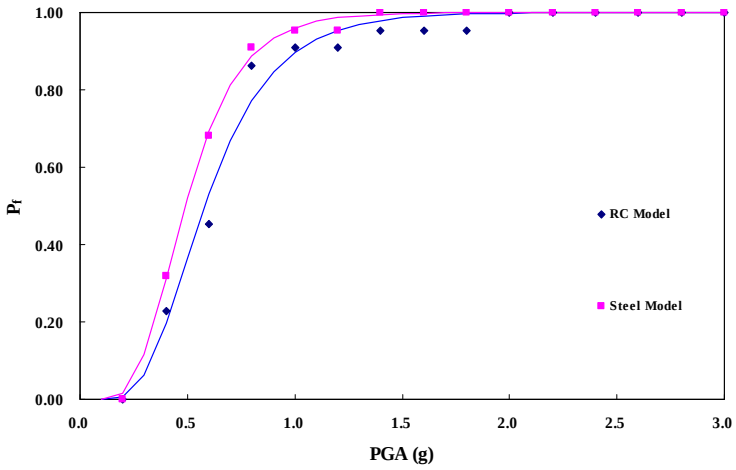

(a) 5-Story

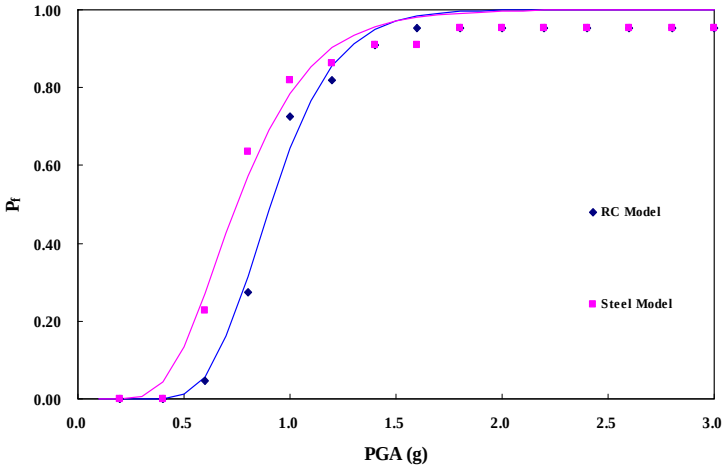

(b) 10-Story

Fig. 13 Piping fragilities on the top in the buildings

probability of failure in RC building models was slightly higher than that of failure in steel linear building systems shown in Figs. 13(a)-(d).

9. Conclusions

This paper demonstrated the fragility methodology of the threaded Tee-joint of the piping system installed on the top floor in critical structures. More specifically, this study was targeted to evaluate the piping fragilities by characterizing the effect of linear building systems, 5-story, 10-story, 15-story, and 20-story linear building systems. In order to evaluate the system-level fragilities corresponding to the first leak damage state, the floor acceleration time histories were

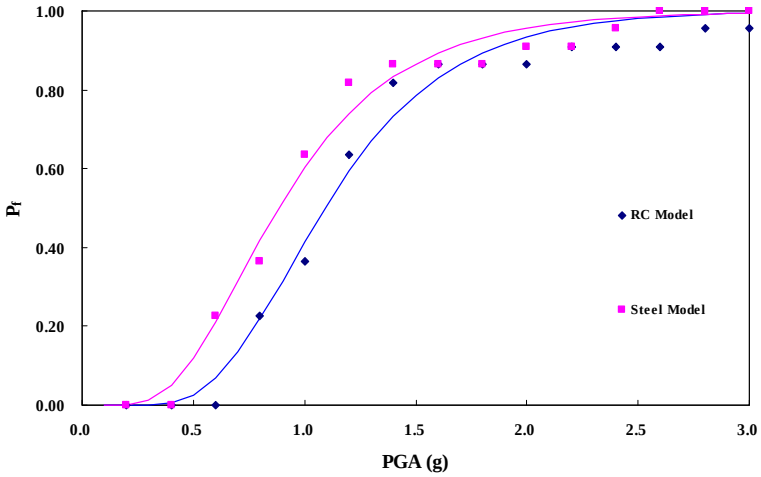

(c) 15-Story

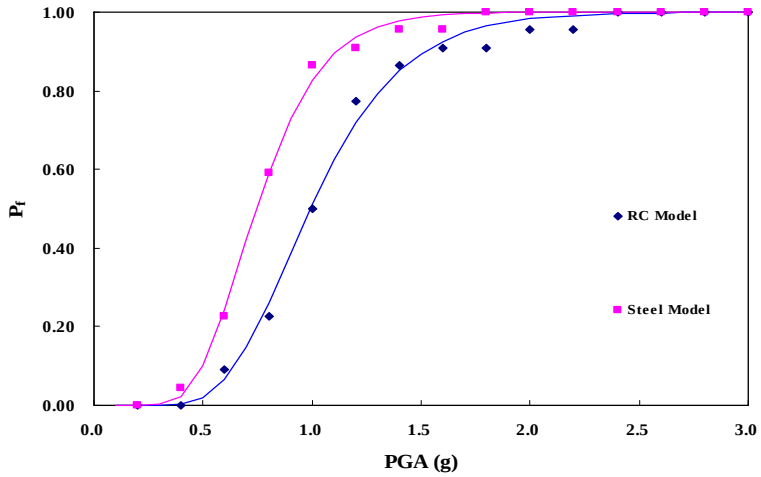

(d) 20-Story

Fig. 13 Continued

obtained from the 22 real earthquake ground motions normalized to same PGA levels from 0.2g to 3.0g at the top floor in each building system and conducted the simulation for complete piping system configurations.

According to these fragility analyses, the piping system on the top floor in 5-story RC and steel building models were most vulnerable, whereas the piping system on the top floor in 15-story building model showed lower fragilities. It can be explained that the response spectral accelerations were significantly different for each building model at the second mode of the piping system. The fragilities in steel building models also showed greater tuning with the piping system than those of RC building models. It indicates that the fragilities of the piping system in steel building system can provide conservative estimation. In addition, the fragility of piping system on

the top floor in the building models increased considerably the failure of piping system at the threaded Tee-joint rather than system level fragility of piping system using ground level excitations. Therefore, the natures of changes in fragility curves were likely to vary at different types of the building systems. Finally, the story height in buildings could result in decrease of the tuning between the buildings and the piping systems. However in some cases, this phenomenon could be in reverse: the story height in buildings can increase the tuning between the buildings and the piping systems.

Acknowledgements

This work was supported by the National Research Foundation of Korea (NRF) grant funded by the Korean government (MEST) (No.2011-0028531)

References

ASME (2004), Rule for Construction of Nuclear Facility Components, ASME Boiler and Pressure Vessel Code, Section III, American Society of Mechanical Engineers.

Bachman, R., Bonowitz, D., Caldwell, P.J., Filiatrault, A., Kennedy, R.P., McGavin, G., and Miranda, E. (2004), "Engineering Demand Parameters for Nonstructural Components", *ATC-58 Project Task Report-ATC*, Redwood City, California.

Bachman, K., Kennedy, R. and Porter, K. (2006), "Developing Fragility Functions for Building components for ATC-58", Applied Technology Council.

Dow, J. (2010), "Testing and Analysis of Iron and Plastic T-joint in Sprinkler Systems", NEESR-GC: "Simulation of the Seismic Performance of Nonstructural Systems", http://nees.org/site/oldnees/filedir_2/REU2009_Dow_Paper.pdf

Ghosh, J. and Padgett, J.E. (2012), "Impact of multiple component deterioration and exposure conditions on seismic vulnerability of concrete bridges", *Earthquakes and Structures*, **3**(5), 649-673.

Ju, B.S., Taninada, S.T. and Gupta, A. (2011), "Fragility analysis of threaded T-joint connections in hospital piping systems", *Proceedings of the ASME 2011 Pressure Vessel and Piping Division Conference*, Baltimore, Maryland, USA.

Kafali, C. and Grigoriu, M. (2003), "Fragility analysis for nonstructural systems in critical facilities", *Proceedings of Seminar on Seismic Design, Performance, and Retrofit of Nonstructural Components in Critical Facilities*, ATC-29-2, Newport Beach, California.

Kircher, C.A. (2003), "It makes dollars and sense to improve nonstructural system performance", *Proceedings of Seminar on Seismic Design, Performance, and Retrofit of Nonstructural Components in Critical Facilities*, ATC-29-2, Newport Beach, California.

Maragakis, E., Itani, A. and Goodwin, E. (2003), "Seismic behavior of welded hospital piping systems", *Proceedings of Seminar on Seismic Design, Performance, and Retrofit of Nonstructural Components in Critical Facilities*, ATC-29-2, Newport Beach, California.

Mazzoni, S., Mckenna, F., Scott, M. H., Fenves, G. *et al.* (2006), "OpenSees Command Language Manual", OpenSees, 2006, http://opensees. berkeley.edu/.

NFPA-13 (2007), Standard for the installation of Sprinkler System, National Fire Protection Association, MA, 2007 Edition.

OpenSees (2011), Open System for Earthquake Engineering Simulation, http://opensees. berkeley.edu/.

Pagnini, L.C., Vicente, R., Lagomarsino, S. and Varum, H. (2011), "A mechanical model for the seismic vulnerability assessment of old masonry buildings", *Earthquakes and Structures*, **2**(1), 25-42.

PEER-NRG NGA (2009), Pacific Earthquake Engineering Research Center: NGA Database,

http://peer.berkeley.edu/nga/.

Reitherman, R. and Sabol, T.A. (1995), "Northridge earthquake of January 17, 1994: reconnaissance report-nonstructural damage", *Earthquake Spectra*, EERI, **11**, 453-514.

Reitherman, R. (2009), "Nonstructural Earthquake Damage", Construction of University for Research in Earthquake Engineering (CUREE), http://www.curee.org/image_gallery/calendar/essays/2010-CUREE_excerpt.pdf.

SMACNA (2003), *Seismic Restraint Manual Guidelines for Mechanical Systems, Sheet Metal and Air Conditioning Contractors*, National Association, Inc.

Wood, R.L. and Hutchinson, T.C. (2011), "Effects of ground motion scaling on nonlinear higher mode building response", Structural Systems Research Project Report Series, Department of Structural Engineering, University of California, San Diego, La Jolla, California.